NEW UPGRADING PROCESS FOR HEAVY OIL USING IRON/ACTIVE CARBON MIXTURE CATALYST

S.Terai, H.Fukuyama, S.Sawamoto, K.Ootsuka
Technology Research Center, Toyo Engineering Corporation
1818 Fujimi,Togo,Mobara,Chiba,297-0017,JAPAN

K.Fujimoto
Department of Applied Chemistry, School of Engineering
The University of Tokyo, Hongo, Bunkyo-ku, Tokyo,113-0033,JAPAN

Key words: hydrocracking, vacuum residue, pyrite/active carbon

Introduction

There are a lot of works and efforts on heavy oil upgrading process. Among them, hydrocracking process converts heavy oil into valuable distillable product minimizing coke formation by using catalyst which may be expensive in some cases and adopting very much high hydrogen pressure which may result in high cost. This paper introduces a mixture of pyrite and active carbon (AC) catalyst which may have advantages over supported metal type in catalyst preparation. The mixture catalyst enabled hydrocracking of vacuum residue (VR) under relatively low hydrogen pressure (7.0-10MPa). The effectiveness of the mixture catalyst on hydrocracking reaction was examined in relation to AC pore structure. The kinetics of reaction using lumping model was also studied to envisage the function of the mixture catalyst.

Experimental

Hydrocracking of VR of which properties are shown in Table 1 was carried out in a one-liter semi-batch magnetically stirred autoclave under constant hydrogen flow rate. Reaction conditions were as follows; VR charge 300g, hydrogen pressure 7.0-10MPa, reaction temperature 415-445°C.

Gaseous products were analyzed by gas chromatography and hydrogen sulfide by detecting tube. The content of naphtha (IBP-171°C), kerosene (171-232°C), gas oil (232-343°C), vacuum gas oil (VGO:343-525°C) and residue (Resid:525°C+) fraction in liquid product were determined by gas chromatography distillation method after separating catalysts and coke by filtration. The amount of coke was determined as toluene insoluble. The hydrocracking conversion was defined as follows; conversion [%] = (100-weight%525°C+ in products)/weight%525°C+ in feed VR.

Results and discussion

Effect of catalyst

The experimental results for various catalyst conditions listed in Table 2 are shown in Figure 1. The coke yield against conversion for each catalyst condition was observed to increase in the order Non-cat.≫Pyrite>Iron/AC≒Pyrite/AC mixture catalyst. In the case of non-catalyst, coke formation began at relatively early stage of conversion and significantly increased in successive reaction. Pyrite could suppress the coke formation only up to the range of 60% conversion. The combination of Iron and AC was examined in order to maximize distillable products with minimal coke formation. Iron supported on AC catalyst showed a good suppression ability of coke formation even through higher conversion level. The mixture of Pyrite and AC also showed the same ability to suppress coke formation as Iron supported on AC catalyst. The usage of mixture catalyst is thought to be advantageous in catalyst preparation

which does not necessitate impregnation with aqueous solution of metal salt, drying, and presulfidation.

Affinity of active carbon with VR

Adsorption tests were conducted to examine the affinity of AC with VR by immersing AC in VR under hydrogen pressure of 10MPa and temperature of 250°C at which cracking was expected not to occur. The quantity of adsorption on AC was defined as weight increase of AC after washing AC with toluene using Soxhlet extraction and vacuum drying. The degree of deasphaltene was calculated as reduction of asphaltene content remained in VR after adsorption. It was observed that AC had affinity with heavier fraction, especially asphaltene.

In order to investigate the relationship between AC pore structure and affinity with asphaltene, the adsorption tests in the same manner as above were carried out differing pore volume and mesopore ratio of AC in the order AC(C)>AC(A)>AC(B). As shown in Figure 2, AC(C) with well grown mesoporous structure exhibited the highest adsorption selectivity to asphaltene.

AC pore structure and Hydrocracking

The influence of AC pore structure on hydrocracking was studied. As shown in Figure 3, it was possible to attain higher conversion with less coke yield with AC which developed more mesoporous structure. From these experimental results, the hydrocracking in the presence of Iron/AC catalyst can be summarized as follows.

- Free radical intermediates are initially generated by thermal cracking of VR.
- Such intermediates are adsorbed on active carbon surface.
- Adsorbed intermediates are hydrogenated and stabilized by Iron and then desorbed from the active carbon surface.
- In the course of this reaction, AC with mesoporous structure provides free radical intermediates with proper sites for adsorption preventing them from polycondensing.

Kinetic study

Kinetic study was carried out to clarify the function and to quantitatively observe activity of catalysts for hydrocracking of VR. Reaction model using lumping species adopted here is illustrated in Figure 4. Residue fraction (525°C+) was classified into saturates (Satu), aromatics (Aroma), resins (Resin) and asphaltenes (Asp) by the method based on ASTM D4124-84 and products were grouped into Lo (Gas, Naphtha, Kerosene, Gas Oil),VGO and Coke. Each reaction path was fitted with experimental data by assuming first-order reaction. The comparison between calculated (lines) and experimental (keys) results for pyrite and pyrite/AC mixture are shown in Figure 5 (A) and (B), respectively. The agreement between calculated and experimental results are fairly good for both cases. The temperature dependence of reaction rate constants for pyrite and pyrite/AC mixture are shown in Figure 6 (A), and (B), respectively. Rate constants for cracking reaction to lighter products (Gas, Naphtha, Kerosene, Gas Oil) and condensation reaction (resins to asphaltenes) of pyrite catalyst were observed to be much sensible to temperature than those of pyrite/AC mixture catalyst. This suggests that pyrite catalyst tends to promote cracking reaction producing relatively lighter products on the one hand, and polycondensation producing asphaltene and finally coke on the other hand. However, pyrite/AC mixture catalyst proceeds reactions keeping middle fractions in products and restricting polycondensation of heavy components such paths from resins to asphaltene and asphaltene to coke. Thus the effectiveness of pyrite/AC mixture catalyst was also verified by this kinetic study.

Conclusions

The pyrite/AC mixture catalyst which is simple in preparation showed excellent effectiveness in hydrocracking of VR with the following results.

- AC with well grown mesoporous structure exhibited the highest adsorption selectivity to asphaltene.
- It was possible to attain higher conversion with less coke yield by using AC which developed more mesoporous structure.
- Kinetic study of reaction by lumping model also verified the effectiveness of pyrite/AC mixture catalyst.
- Hydrocracking was possible under relatively low hydrogen pressure by using mixture catalyst.

Thus pyrite/Active Carbon mixture catalyst was proved to be effective for upgrading of heavy oil with low hydrogen pressure condition.

Acknowledgments

This work has been carried out as a research project of the Petroleum Energy Center with the subsidy of the Ministry of International Trade and Industry, Japan.

Literature

Nakamura,I. and Fujimoto,K., PREPRINTS, Div. of Petro. Chem., ACS, 39(3),1994.

Table 1
Properties and Composition of Vacuum Residue

Feedstock			Middle East Blend VR
Density(15°C)		[g/cm3]	1.0334
Total Sulfur		[wt%]	4.02
Total Nitrogen		[wt%]	0.53
CCR		[wt%]	22.4
Metal	Ni	[wtppm]	53
	V	[wtppm]	180
C/H	C	[wt%]	84.8
	H	[wt%]	10.2

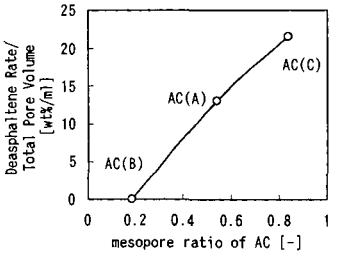

Figure 2 Mesoporous structure and adsorption selectivity of asphaltene

Table 2
Tested Catalysts

Case	Catalyst
1	Non Catalyst
2	Pyrite
3	Iron supported on AC Cat.(Iron/AC)
4	Pyrite/AC Mixture Cat.

AC:Active Carbon

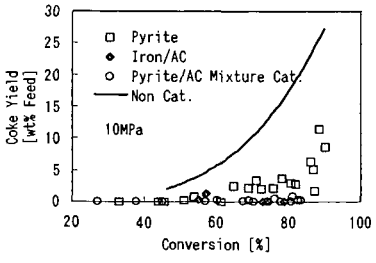

Figure 1 Hydrocracking results with several catalysts

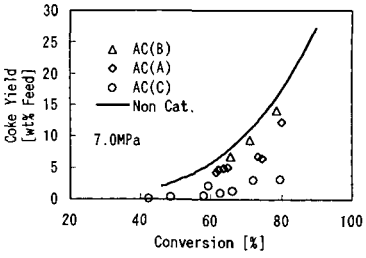

Figure 3 Relationship between porosity of AC and coke yield

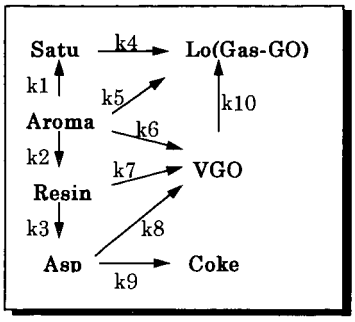

Figure 4 Reaction Model

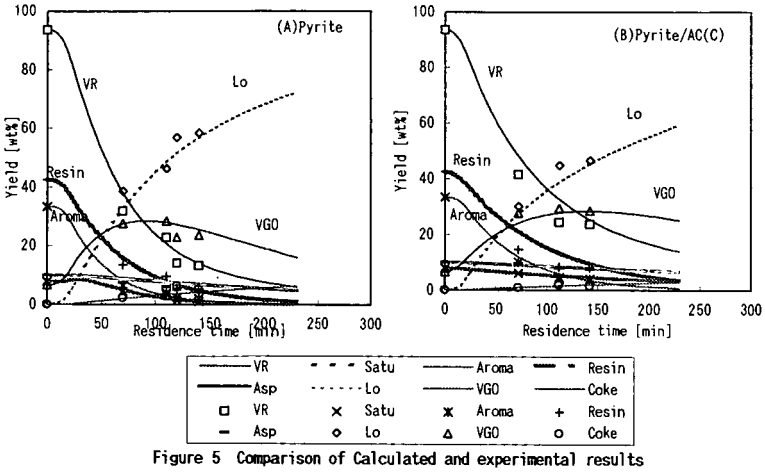

Figure 5 Comparison of Calculated and experimental results

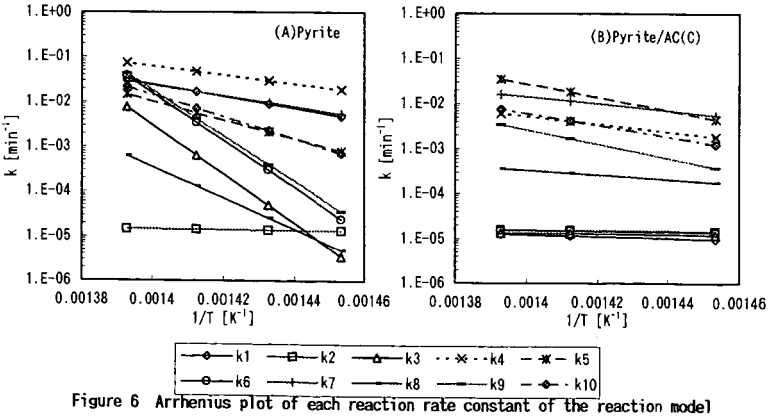

Figure 6 Arrhenius plot of each reaction rate constant of the reaction model